Conducting Spectra-Spatial Investigations on the Big Island of Hawaii as a Lunar Surface Analogue

Hao Wang[1], Krystal Arroyo-Flores[2], and Frances Zhu[3]
University of Hawai'i at Mānoa, Honolulu, Hawai'i, 96822, USA

In order to evaluate the likeness of the Big Island as a lunar surface analogue to simulate lunar mission operations, this project is proposed to conduct spectra-spatial investigation with a visible and near-infrared (VNIR) spectrometer. The field spectral measurements are compared to the returned lunar samples and the lunar simulants. In this project, a procedure is developed to collect spectra in analogue field tests and a quantitative analysis of the material likeness of ground samples at the Big Island planetary analogue field site to each other (sample consistency) and to Apollo samples (lunar similarity) is conducted. This comparative analysis has provided valuable insights into the consistency and similarity of the analogue to the lunar surface, which will benefit the development of scientific and technological investigations intended for the lunar surface missions.

I. Nomenclature

ρ	=	Pearson's correlation coefficient
cov	=	covariance
σ	=	standard deviation
E	=	expectation
X,Y	=	vector of reflectance values

II. Introduction

The lunar South Pole region is a hotspot of exploration in the Artemis era of human lunar exploration, especially the Permanently Shadowed Regions (PSRs). The main scientific interest is to quantify water ice that was confirmed on the surface of the Moon's South Pole, from which the Artemis program can extract oxygen and hydrogen for life support systems and fuel [1]. However, the extreme contrasting conditions in this uncompromising area, including extreme temperatures and lighting variability, make it challenging for humans to land, live, and work. Unlike where Apollo missions landed, it is not exactly sure what the terrain in the Moon's polar regions will be like.

Spectroscopy is one of the most widely used methods in planetary science for both remote sensing and in-situ measurement. The unique spectral features in measurements enable us to identify the ingredients by comparing the measured spectra to the references in a database. Some astonishing discoveries would not be possible without spectroscopy, such as the confirmation of water ice on the Moon [1, 7]. Future space missions in the lunar South Pole region, the hotspot in the Artemis era of human lunar exploration, will employ spectrometers onboard the rover VIPER to detect water ice and understand the distribution of natural resources [8]. The identification accuracy partly depends on the search algorithm of the database and how noisy the spectral measurements are. However, unlike laboratory measurements, in space missions, an insufficient number of samples or contamination of other chemical compositions in the field of view could make spectral data noisy and challenging to identify. Many other factors can significantly affect the measurement reading, such as peak shift due to temperature change, particle size distribution, light source, etc., especially for a location with very limited information, like the lunar South Pole region. Thus, it is critical to

[1] Postdoctoral Researcher, Hawai'i Institute of Geophysics and Planetology, and AIAA Young Professional.
[2] Graduate Assistant, Department of Earth Sciences.
[3] Assistant Professor, Hawai'i Institute of Geophysics and Planetology, and AIAA Young Professional.

identify and evaluate realistic analogue environments on Earth and conduct field tests of surface exploration activities before the mission.

Planetary analogues are sites on Earth used in place of locations with similar environments in space, providing a more convenient way to conduct mission field tests and rapidly develop technologies to eventually be deployed in space. The Hawaiian Islands have many potential analogue sites for lunar surface rover exploration, especially on the Big Island. Analogue tests have been crucial in advancing our understanding of the challenges and potential solutions for deep space exploration. The Rover-Aerial Vehicle Exploration Network (RAVEN) has been field tested at Holuhraun, Iceland [15]. Mauna Kea Volcano, Hawai‘i, Kīlauea Volcano, Hawaii, and Potrillo Volcanic Field, New Mexico, have all been used as analogues for planetary studies [10, 11, 12]. Among these analogue tests, NASA has conducted a series of major Moon and Mars analogue field testing campaigns at Mauna Kea on the Big Island from 2010 to 2012 [10, 12, 14]. These analogue tests involve the simulation of operation and experiments in lunar and Martian environments, allowing both scientists and engineers to study the unique conditions and operational complexities they may encounter during future missions. These tests have provided valuable insights into operations strategies, In Situ Resource Utilization (ISRU) construction, instruments, planetary geological field work, and communication in planetary surface missions [9-15]. However, although local material, terrain, logistics, and accessibility are considered in the NASA campaign plan, and the Pu‘uhaiwahine site on Mauna Kea Volcano is claimed to provide terrain features and volcanic tephra that reasonably simulated lunar regolith physical and mineral characteristics [12, 14], there is no unified evaluation standard of the similarity between planetary analogues and the real lunar surface. Furthermore, there is no analogue evaluation targeting the spectral prospecting water ice in the lunar South Pole region. To the best of our knowledge, there is no quantified investigation data available in the public domain.

This research aims to evaluate the likeness of the Big Island as a lunar surface analogue for future lunar surface exploration activities via spectra-spatial characterization. The final products include correlation matrices along with their corresponding heatmaps. One matrix displays the correlation between each analogue sampling site, while another represents the correlation between the analogue sampling sites and lunar returned samples. A third matrix is dedicated to the correlation between the analogue sampling sites and lunar simulants. In addition, two tables summarize the analogues with the highest correlation coefficients for each reference spectrum in the library. A plot of correlation coefficients versus relative distance is also provided to visually illustrate the relationship between correlation and geographical distance. The outcome of this research will benefit future lunar surface exploration, like deploying autonomous lunar rovers to detect water ice or simulating astronaut geological surveys in the South Pole region.

In this research, our team has made significant contributions in several key areas. Firstly, an effective procedure is developed to collect spectra in analogue field tests. With collected data, a quantitative analysis of the material at the Big Island planetary analogue field site, located near the Onizuka Visitor Center, is conducted. The spectral measurements in our field data with various samples, including analogue samples, lunar regolith, and lunar simulants, are compared to evaluate the similarity of the field site to the lunar environment. This comparative analysis has provided valuable insights into the lunar surface analogue, which will benefit the development of lunar surface autonomous prospecting and other rover/astronaut exploration techniques.

Section III outlines the research methods employed, including spectroscopy, sensor technology development, analogue site selection, data-gathering field campaign, and data analysis. Section IV introduces the research outcomes, featuring correlation matrices and their accompanying heatmaps, which reveal the relationships between the analogue field site sample locations and existing lunar simulants and returned lunar samples. Section V presents a comprehensive discussion with a focus on error analysis. Finally, conclusion and future work discussion are presented in Section VI, highlighting the study's main findings and the future plan.

III. Experiment Methods

This section describes the use of spectroscopy, construction of a spectra-spatial sensor suite, selection of analogue field sites, data acquisition in the field, and data processing employed for this project. The order of these elements also follows the chronological progression in which they were completed.

A. Spectroscopy

A Visible and Near-Infrared (VNIR) spectrometer supplies both field and laboratory measurements used in our analysis. The portable spectrometer (Fig. 1) used for this study is an ASD FieldSpec®4 Standard-Res from Analytical Spectral Devices, Inc., with a spectral range from 350 - 2500 nm and 5 nm spectral resolution.

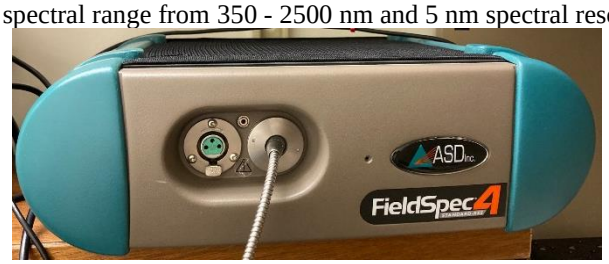

Fig. 1 The Portable Spectrometer

Spectroscopy is widely used to detect and identify ingredients for both remote sensing and in-situ measurement with unique spectral reflectance and absorption features in measurements. Spectral observations of the lunar surface in the VNIR wavelength range contain a wealth of important mineralogical information on the lunar terrain, indicating both signatures and proportions of distinct minerals [22, 23]. Meanwhile, portable spectral imaging technology in various wavelength ranges is mature and currently employed in the study of planetary science [11, 13]. The ASD FieldSpec® 4 Hi-Res is a widely used and discussed VNIR spectrometer in the lunar exploration field [24, 25]. In the Artemis era, in-situ spectral measurements will be collected to identify and characterize the lunar terrain, specifically the south pole region under a wide range of conditions, such as lighting, temperature, and viewing angles. In this research, the VNIR spectrometer serves as a powerful tool to investigate the volcanic analogue terrain with potential water ice presence. Although the existence of water ice is confirmed by the remote sensing data, the details - such as exact locations and abundance - remain unknown [1]. Water ice exhibits distinctive absorption features within this wavelength range. However, the terrain background and environment conditions need to be considered to distinguish its presence from other materials. To accurately identify the water ice and estimate its abundance, it would be critical to conduct multiple analogue field tests of the surface exploration rover and onboard instruments under various simulated lunar conditions before the launch. Thus, it holds significant implications to evaluate the likeness of the volcanic analogue site to the real lunar terrain. Instead of identifying individual components, our approach leverages the spectral measurements collected from different sample sites throughout the analogue field site to characterize the terrain by comparing the field measurements to lab measurements of lunar simulants and lunar returned samples in the spectral library. The results will not only benefit the evaluation of the lunar surface analogue, but also serve as reference spectra for the estimation of water ice abundance in the targeted samples. Fig. 2 is a sample raw spectral measurement collected in the field test.

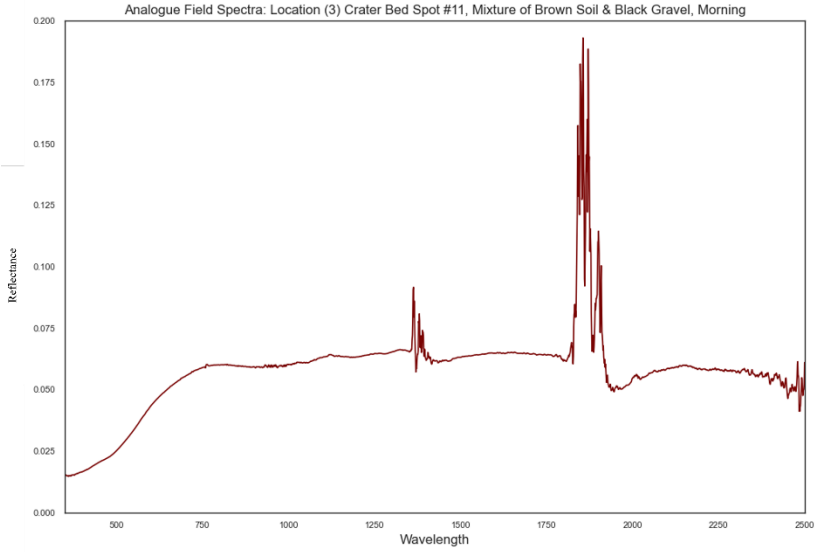

Fig. 2 Sample Spectrum Collected in The Field

B. Sensor Suite

Although the ASD FieldSpec is already designed to be used by human operators to gather measurements in the field, a suite is designed to incorporate additional sensors and improve the consistency of point data gathered throughout the campaign. For this initial iteration of the sensor suite, two sensors were chosen to supplement the spectrometer: the GT-U7 Global Positioning System (GPS) Module + Patch Antenna, and the GY-521 MPU-6050 Inertial Measurement Unit (IMU). These two sensors measure position, rotation, acceleration, and temperature and can be wired simultaneously to one control board for both power and data connections. The control board used in the design is an Arduino UNO Rev3 (see Fig. 3).

Requirements driving the sensor suite design included the incorporation of ASD-provided spectrometer accessories (field backpack, rechargeable field battery, laptop processing computer, and fiber-optic cable pistol grip), as well as increased measurement consistency and ease of operability while out in the field. The field backpack houses the main spectrometer body, the connected battery, a spare battery, and a sling board, which holds the laptop computer suspended in front of the operator. To obtain the most accurate spectral measurements possible, the fiber optic spectrometer cable must be held at a consistent angle to and distance from each target sample, and must also be regularly pointed at a white reference panel to re-calibrate the instrument for any changes in environmental light. To minimize fatigue and error from manually holding the cable above each target, a "Sensor Staff" is designed which would both hold all of the sensor apertures at consistent positions and angles relative to each other and the target point, and act as a hiking aid to the operator.

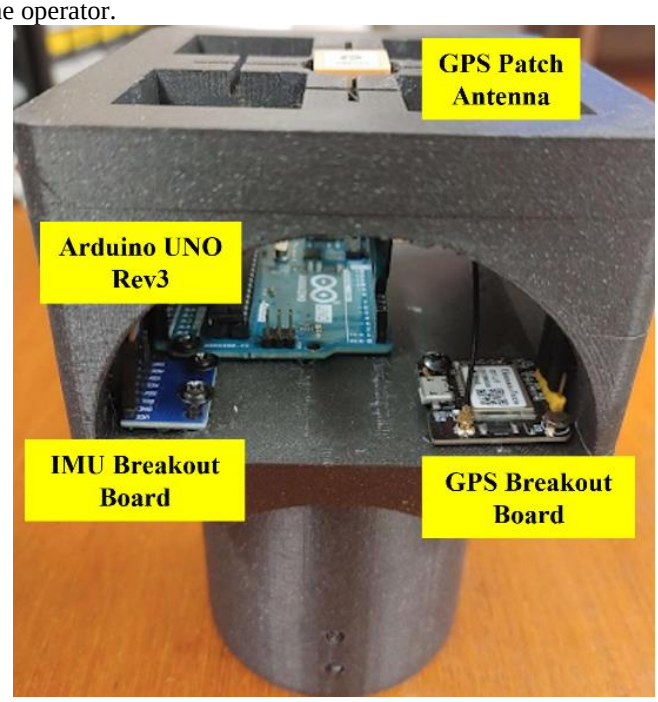

Fig. 3 3D-Printed Sensor Box Housing the IMU, GPS, and Arduino.

The staff is constructed from a PVC pipe approximately 4 ft in length and 1.25 inches in diameter, both chosen for a comfortable height and grip. A 3D-printed block-shaped housing sits on the top of the pipe with a press fit (Fig. 4). The housing maintains a radially symmetrical silhouette while protecting the Arduino, IMU, and GPS printed circuit boards. The GPS patch antenna is mounted within the top face of the housing in the center of the staff, for maximum line of sight to facilitate a valid location. A power and data cable connects the Arduino directly to the laptop computer, passing the appropriate voltage through it to each sensor and streaming their measurements back to the computer.

On the lower end of the staff is a mount which holds the fiber optic cable grip at a constant 0-degree angle to the staff (90 deg to the ground surface). The spectrometer has a 25-degree field of view and therefore an approximately 1:2 ratio of the target diameter to the distance from the sample (Fig. 5). For proper white reference calibration, the target diameter must be no greater than the diameter of the white reference panel used. Because our panel is five inches in diameter, this constraint resulted in a mount height of approximately one foot from the bottom of the staff. The mount is also designed as a horizontal arm, holding the pistol grip such that the fiber-optic cable aperture is approximately seven cm away from the staff body, so as not to obstruct the field of view (Fig. 6).

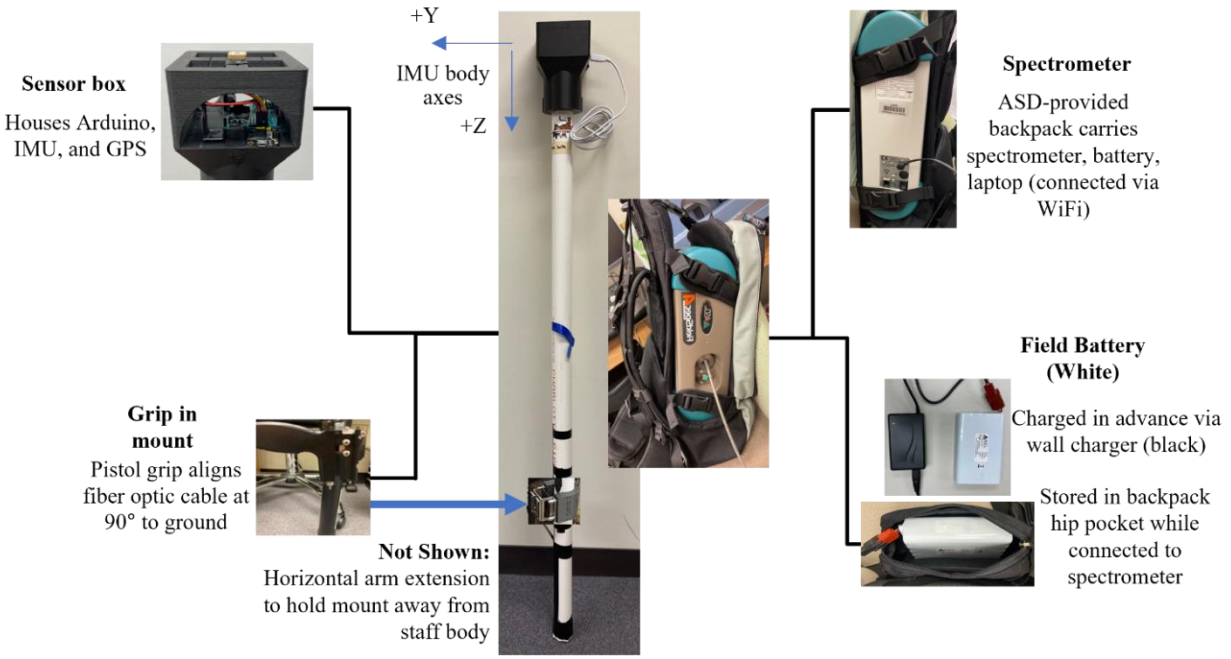

Fig. 4 Sensor Suite Diagram Illustrating Positions of Components Either on the Sensor Staff or within the Spectrometer Backpack

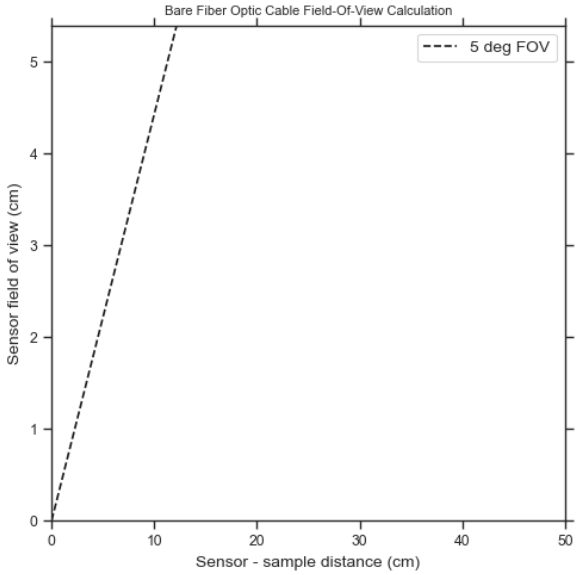

Fig. 5 FieldSpec®4 Field of View Diagram

As the spectrometer receives power from the field battery held in the backpack's hip pocket and transmits data to the computer via a dedicated WiFi connection, the sensor cable and fiber optic cable are the only two physical connections between the backpack and the staff. An optional trigger button cable can be connected to the spectrometer and held anywhere that is comfortable for the operator to reach, but is not necessary for operation. The fiber optic cable is the shorter and more fragile of the two required cables, and thus is the limiting factor for how far the operator can safely stand from the target measurement.

A second staff was constructed from a slightly-smaller-in-diameter PVC pipe to hold the white reference panel both at a constant distance in between the fiber optic cable and the target surface, and also at a constant 90-degree angle (perpendicular) to the cable aperture, providing stability during calibration.

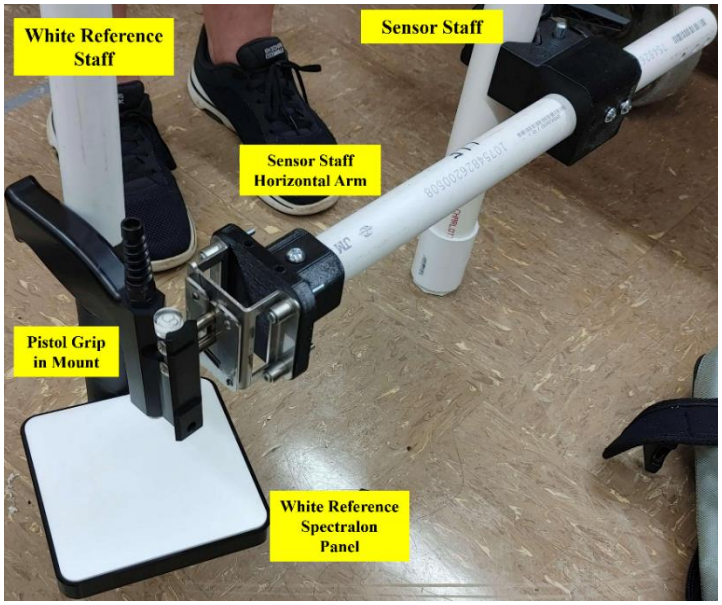

Fig. 6 Sensor Staff and White Reference Staff Configuration

C. Analogue Field Sites

Prior research from the Pacific International Space Center for Exploration Systems (PISCES) characterized the chemical composition of basalt samples from multiple sites in Hawai‘i, from which they determined that Pu’uhaiwahine (19°45'33"N, 155°27′22″W) is one of sites with the most chemically similar basalt to lunar samples are[4, 5] (Fig. 7). A research permit application was submitted to the Hawai‘i Department of Natural Land and Resources (DLNR) for the former site, the Pu‘uhaiwahine valley on Mauna Kea. The site is a valley located west of the Mauna Kea Visitor Information Station (VIS). While the true summit of Mauna Kea has an altitude of 13803 ft, the VIS sits at 9200 ft (approximately 66.6% max elevation). Our area of interest as submitted for the permit is close to where NASA conducted a previous analogue campaign.

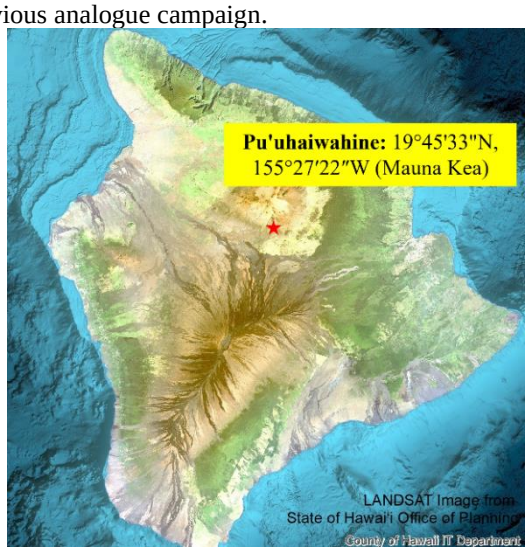

Fig. 7 Analogue Field Site Location

Site characteristics that geologically and spectrally emulate the lunar surface include 1) Surface water ice is lower than 30% that mixed in soils; 2) Surface ice is isolated or sporadic, or desiccated land can be easily accessed; 3) Soil will be anorthositic or basaltic with less aqueous alteration and less organic matters; 4) Slopes limited to 30 degrees; 5) Primarily regolith terrain with minimal bulk obstacles. In this field test, our team focused on sampling around Pu’uhaiwahine at four distinct locations, identified as (1) Power Station, (2) Between Two Cinder Cones, (3) Crater Bed, and (4) Crater Slope (see Fig. 8 labels: ‘PS,’ ‘Spiral,’ ‘Crater,’ and ‘Slope,’ respectively).

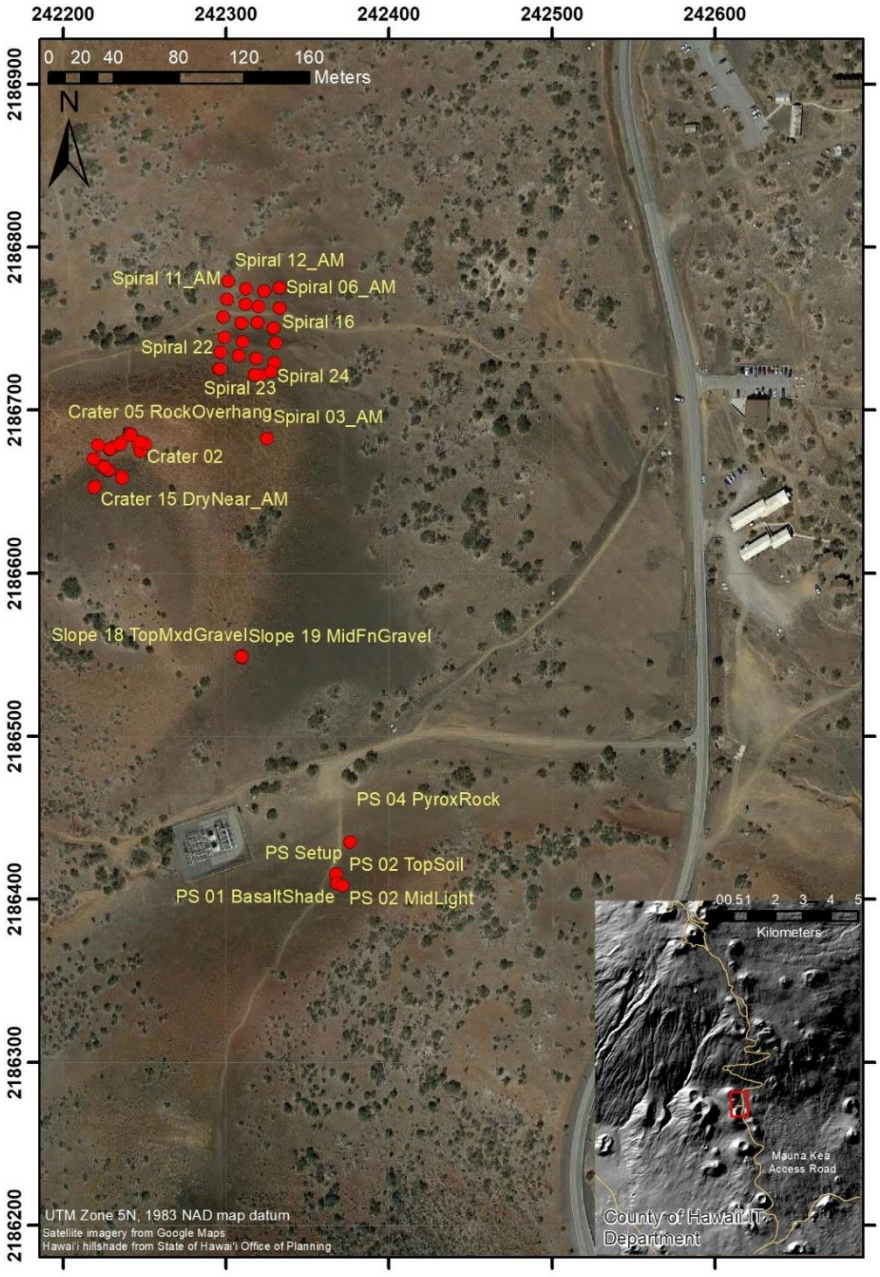

Fig. 8 Sampling Sites on Mauna Kea: The four Locations are differentiated by unique label prefixes among the clusters of coordinate points. The location of the research area lies along the Mauna Kea Access Road and is outlined in red in the inset.

Three primary sampling strategies are employed: (1) Spiral Pattern: this approach involves following a spiral pattern originating from the center of an open area. Along this pattern, 12 spots were sampled, each separated by ten meters, unless the location was entirely inaccessible. Ten additional spots were later sampled in a similar grid-like pattern as light changes permitted, for a total of 24 unique sample spots measured in Location (2) (Fig. 9 (a)). (2) Representative Sampling: For the remaining unique samples in the other three locations, spots were selected based on visual cues such as variations in color, particle size, and mineral mixing, aiming to capture representative samples of the terrain (Fig. 9 (b)). (3) Lighting Discrepancy Revisits: As part of our third strategy, certain sampling spots at different locations were revisited in the morning after first identifying them in the previous afternoon. This allowed us to collect measurements under different lighting conditions, enabling a more comprehensive collection of the spectral data.

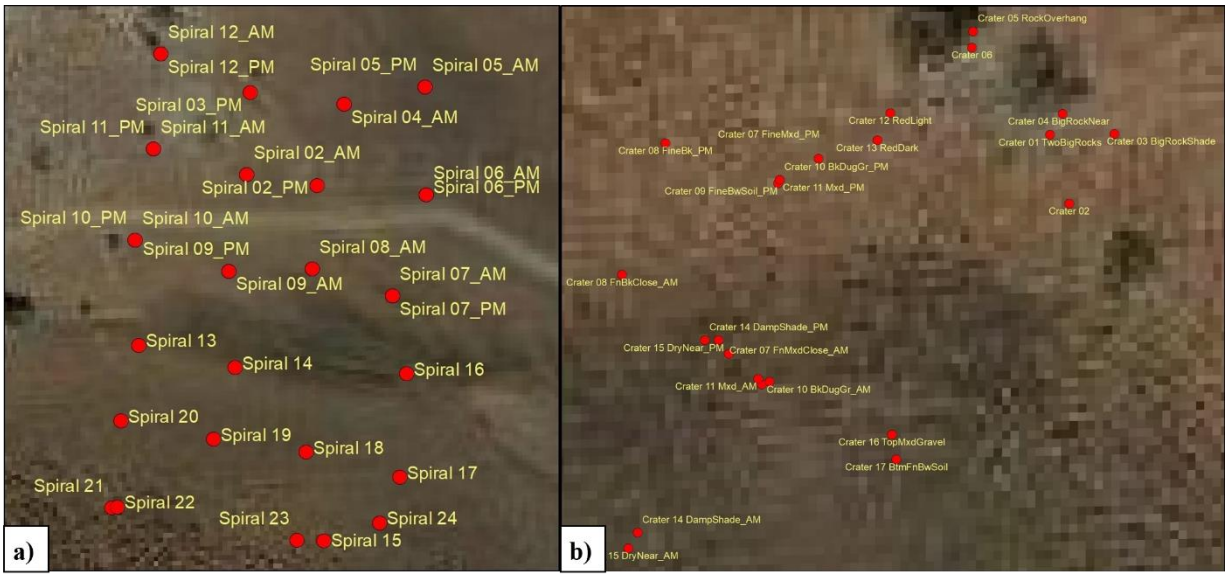

Fig. 9 Close-ups of sample spot distribution in a) Location (2) and b) Location (3).

The sampling sites were carefully selected to encompass a variety of terrain features. On the first morning (Day 1 Morning), Location (1), the Power Station site, was visited to measure frost or ice mixed with surface soil. This initial choice was motivated by a prior observation of frost beneath a rock in this location. In the afternoon of the same day (Day 1 Afternoon), Location (2) Between Two Cinder Cones was sampled, following a spiral or grid-like pattern. The next morning (Day 2 Morning), this site was revisited to collect measurements under more favorable dawn lighting conditions. In the afternoon of Day 2, measurements were taken at Location (3) Crater Bed, with sampling spots picked ad hoc according to likelihood of frost accumulation and regolith variety. On the final day of sampling (Day 3 Morning), Locations (1) and (3) were revisited to look for possible frost and to again gather measurements under more favorable lighting conditions. A final few samples were measured at Location (4) on the Crater Slope, where the regolith appeared flatter and more consistent. For each sampling spot, multiple consecutive measurements were taken to average together during data analysis to reduce errors. Across the entire field site, four samples were measured at Location (1), 24 samples at Location (2), 17 samples at Location (3), and three samples at Location (4). 12 samples from Location (2) and 13 samples from Location (3) were measured during both morning and afternoon sessions, resulting in a total of 73 distinct sampling instances of 2 - 9 individual measurements each.

D. Data Gathering Procedure

A well-defined and easy-to-implement procedure is essential to ensure accurate and reliable data collection in field spectral characterization. The following steps outline the procedure for a field VNIR spectrometer with specific instructions for setup, data acquisition, and optimization:

Setup:

1) Power On Spectrometer: Connect charged field battery to the spectrometer and flip the Power Switch to ON. The spectrometer must warm up for a minimum of 20 minutes to stabilize its readings.
2) Connect Laptop: Connect the operations laptop to the instrument's internal WiFi network to enable data transmission.
3) Launch Spectrometer Software: Start the RS3 High Contrast program and confirm network connection.
4) Power On Sensors: Connect the combined power and data cable from the Arduino UNO to the laptop. Verify power to the IMU and GPS via on-board LEDs. The GPS can take up to 20 minutes to calibrate its position after establishing line-of-sight.
5) Launch Sensor Software: Start Data Streamer in Excel, connect to the appropriate COM Port, and verify that sensor data is streaming.

Spectra Acquisition:

6) Configure Spectra Save Settings: Set the save folder and naming options in the RS3 Control settings.
7) Clean White Reference: Clean the white reference panel for calibration with compressed air.

8) Position Optics: Place the sensor staff on the ground such that the spectrometer fiber optic cable points directly down at the target. The field operator should orient the staff and their own body such that neither blocks sunlight to the target (see Fig. 10).
9) Position White Reference: Place the white reference staff on the ground such that the panel is in between the fiber optic cable and the target, with the center of the panel centered under the cable aperture.
10) Optimization: Press the 'Opt' button in RS3 to perform optimization and Dark Current measurements. Repeat if necessary.
11) White Reference Calibration: Press the 'WR' button in RS3 to perform calibration. Confirm appropriate WR spectrum within the on-screen display before proceeding. Repeat multiple times if necessary.
12) Remove White Reference Panel: Save one or more white reference measurements carefully rotate the panel out from underneath the spectrometer aperture without disturbing either the sensor staff or the target.
13) Wait for Stabilization: Allow the display to stabilize to a constant spectrum for the target.
14) Save Spectra: Set a new file save name if desired and save multiple consecutive spectra, allowing a couple of seconds between each.

Fig. 10 Positions of the Field Operator, Sensor Staff, and White Reference Staff for a Field Measurement

IV. Data Analysis Method

The field measurements are processed using ASD software ViewSpec Pro, following a series of essential steps. Initially, noisy measurements are filtered out, and atmospheric water bands are eliminated. Correction operations are also applied to further refine the data. Subsequently, multiple spectra captured for each target are averaged into a single spectrum. The data is then converted from ASD-formatted files into easily readable ASCII text files, and the spectra are saved into arrays for analysis. To assess the relationships between analogue measurements, correlation coefficients are calculated for each pair, resulting in two correlation matrices. Additionally, relative distances between analogue sites are computed based on GPS records and these distances are used to plot the relationship of correlation versus geographical distance. Furthermore, a reference library is established, featuring spectra from selected highland and mare lunar returned samples and simulants. This reference library enables us to compare the analogue measurements with the spectra in the library, leading to the generation of correlation matrices and the identification of maximum correlations for each reference spectrum.

A. Pre-processing ASD FieldSpec Files

The development of the Sensor Suite for this field test combined selected sensor hardware together and made use of both commercial and in-house software to obtain all of the spectral data from the field. The data gathering procedure outlined in the previous section was carried out with the Sensor Suite at the selected analogue field site for each sample spot, with the location of each sample chosen according to one of the previously mentioned sample strategies. The overarching goal was to gather a variety of measurements from both visually similar and varied targets, to improve the likelihood of confirming spectral similarities between the analogue field site and the lunar environment. To this end, each sample spot was chosen ad hoc shortly before measuring it, sometimes according to geographical distribution, as in the spiral/grid pattern followed in Location (2), as well as according to variation in particle size, texture, color, presence of organic matter, likelihood of direct sunlight, and identifiable components. Each spectral measurement saved is stored on the operational laptop as an .asd file, which is a binary format standard to ASD spectrometers, and only readable by ASD processing software. The left side of the flowchart in Fig. 11 illustrates the various steps involved in obtaining the spectra up to this point.

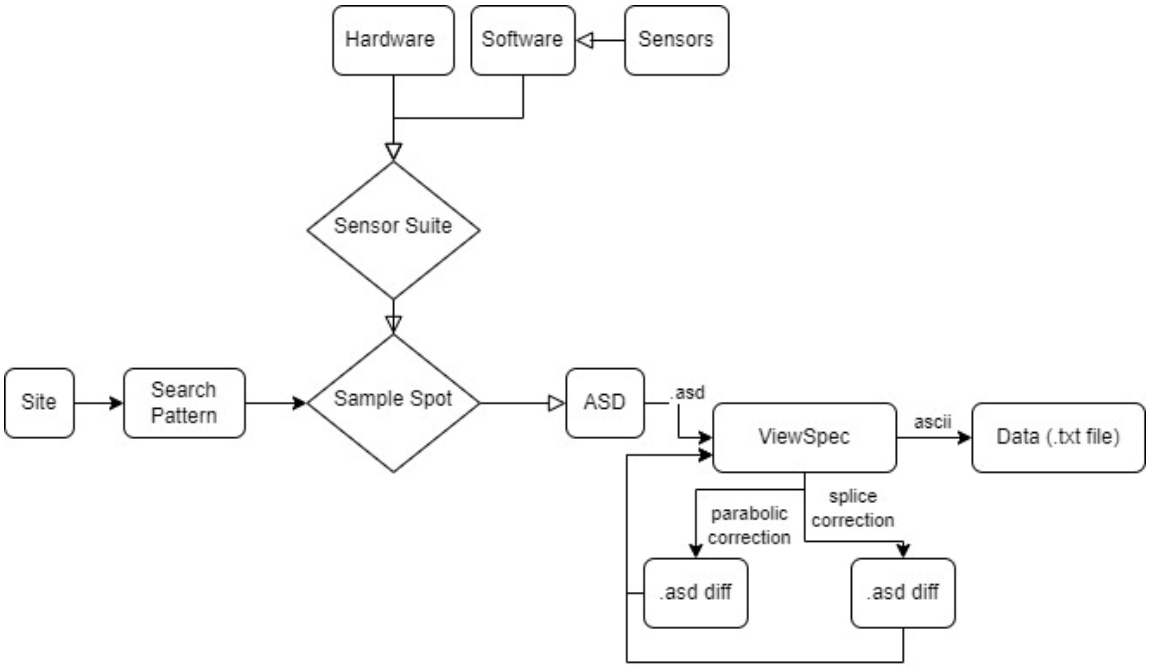

Fig. 11 Data Acquisition and Pre-Processing Flowchart.

The ASD processing software ViewSpec Pro is used for all pre-processing steps of the .asd files before they are exported as .txt files for further post-processing and eventual statistical analysis [31]. The first step in post-processing is to import all of the relevant .asd files into ViewSpec and use their graphing tool to perform an initial filter of the individual spectra by visually inspecting them for files containing significant noise. Noisy spectra data files were due to the field of view moving before RS3 could finish producing a stable average of the target, lighting conditions changing during a measurement, the spectrum saving before performing necessary white reference re-calibration and/or re-optimization, or the data was contaminated by excessive noise, such as high atmospheric moisture or sub-optimal lighting intensities or angles (some noise from atmospheric moisture is expected in known water bands and are accounted for in a later step). Once all excessively noisy data files are removed, each spectra is inspected for variations necessitating correction. The structure of VNIR spectrometers, with three separate detectors, can sometimes lead to bias in the wavelength region specific to the mid-range detector. If a spectrum has this variation, it can be run through either ViewSpec's parabolic correction operation or its splice correction operation. For this study, splice correction was used to correct any variations present. After all files have been corrected, the multiple spectra taken of each target were averaged into one spectra using ViewSpec's Statistics process. This process can produce both a mean spectra and a median spectra, and both were produced and compared for each target sample to select the best representation of noise reduction and measurement stabilization for that sample. The final step in pre-processing is to process all of the single target files (which depending on the previous two steps, can be in .asd, .sco, .md, or .mn file formats) with ViewSpec's ASCII Export operation. This operation converts the ASD-formatted files to easily readable ASCII text files, with configuration options for setting data format (relative Reflectance is the standard), header information, and field separator, among others. The resulting .txt files can be read by many different programs as desired for processing and analysis.

B. Filtering Noise

The data files were processed using python in Jupyter Lab, leveraging packages such as numpy, pandas, and seaborn for specific operations. All of the spectra from the analogue field site underwent noise elimination before they could be used to calculate correlation. For this step, the spectra were plotted and inspected for noise in atmospheric water bands, then specific boundary wavelengths were chosen for each water band to be consistent with both this inspection and standard boundaries used in available toolkits or within industry research. The reflectance values sitting within these band boundaries were dropped from all analogue field files, and the spectra were plotted again to verify the noise elimination (Fig. 12).

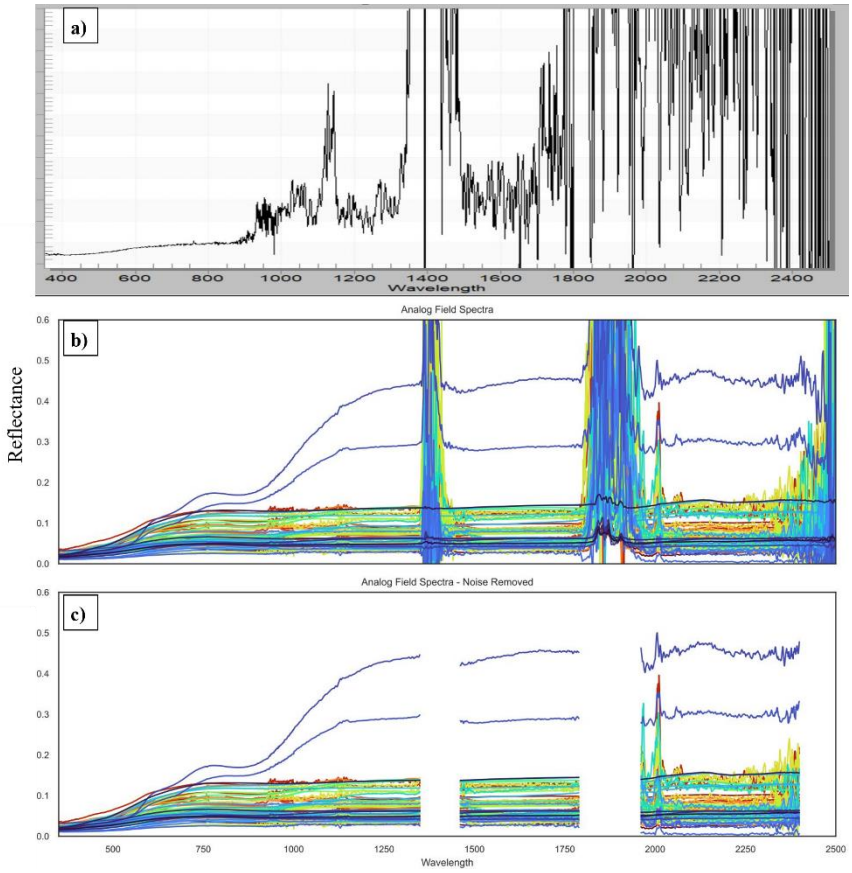

Fig. 12 Analogue Field Data: a) Excessively Noisy Spectrum (Unusable), b) Saved Spectra, c) Spectra with Atmospheric Water Bands Removed.

C. Reference Spectra Selection

To facilitate comprehensive analysis, a dedicated spectral library of lunar simulants and returned lunar samples was established to enable thorough comparisons with field measurements. The reference spectra are selected among all the lunar returned samples and lunar simulants in the RELAB Spectral Database [20] and USGS Spectral Library Version 7 [21], the two widely used databases for planetary science with lunar samples and lunar simulants measurements. This research targets to evaluate the analogue site for future lunar south pole region exploration. The south pole of the Moon is located in the cratered terrain of the southern highlands, and the lunar surface in this region is dominated by anorthosite [26-30]. Thus, the highland samples from Apollo 14 and 16, the highland simulants, and the anorthositic simulants are given priority. A few mare samples from other Apollo missions and mare simulants are also used as a comparison. Meanwhile, since particle size may affect spectral measurements, samples with different size distributions are adopted as reference spectra. Additionally, the amount of data and wavelength range have a significant impact on the correlation calculation. The correlation is calculated only based on the data at the available bands. In our measurements taken in the analogue, there are 1768 points for each field spectra, while the highest count in any of the library files is 356. The lowest ones only have 31 points for each spectra. The correlation might not be accurate with a low amount of data in the spectra being compared. The samples in the spectral library have various wavelength ranges. Although our field measurements are taken in the visible and near-infrared (VNIR) spectral range from 350 to 2500 nm, some samples in the library are only measured in the visible light range and may not contain the important spectral signatures. Thus, the selected samples have at least 352 data points in each spectrum and cover the visible and near-infrared wavelength range. The one exception is the one Apollo 17 sample, which only covers the near-infrared range. The reference files used for this study did not need to be processed for atmospheric noise, but were put through processing operations in python to import their data into pandas DataFrames in similar formats to those formed by the imported analogue field data text files. In particular, all reference files were processed to to align the specific wavelength ranges and values included to those used in the measurements from the ASD spectrometer.

D. Generating Correlation

A correlation matrix is the major tool adopted to assess the degree of similarity among analogue sites as well as between analogue sites and the special profiles in the spectral library, which includes measurements of lunar simulants and actual lunar terrain represented by returned lunar samples. The correlation matrix consists of the correlation coefficients of each pair of measurements. This study used the pandas DataFrame ".corr" method, which by default calculates the pairwise correlation coefficient between each column of a DataFrame, using the Pearson method, which is the standard method for calculating correlation coefficients.

For a long time, statistical correlation coefficients have been used for the quantitative comparison and identification of spectra [17-19]. Library matching is a well-established method in spectroscopy for the investigation of unknown materials, typically performed by cross-correlating the measured spectrum of a material against a validated library of spectra of known materials. The degree of correlation (similarity) is quantified by a calculation of correlation coefficient [16]. By quantifying the correlations between the spectral measurements of each pair of sampling spots, the consistency of the analogue site is evaluated. By quantifying the correlations between the spectral measurements of analogue site and lunar simulants, then between the measurements of analogue site and lunar samples, the fidelity of the lunar surface analogue representation is gauged based on spectral features. One notable aspect of correlation analysis is its ability to account for vertical shifts or biases in the spectra while still presenting an accurate correlation due to its vector calculation nature, which is particularly valuable when lighting discrepancies or other systematic variations exist. The correlation analysis captures the similar patterns of variation, rather than two spectra's absolute values. When measurements are missing at certain wavelength bands, a pairwise deletion is employed in both spectra being compared. This method reduces the influence of missing data on results, allowing the correlation calculation to be primarily based on the available measurements at the desired wavelength bands.

Correlation is a statistical measure that quantifies the degree of relationship or association between two or more variables. There are multiple correlation coefficients. The most familiar one is the Pearson's correlation coefficient, obtained by simply dividing the covariance of the two variables by the product of their standard deviations as in Eq.1, ranges from −1 to 1.

$$\rho_{X,Y} = cov(X,Y)/\sigma_X\sigma_Y = E[(X - E[X])(Y - E[Y])]/\sigma_X\sigma_Y \quad (1)$$

An absolute value of exactly 1 implies a perfect linear relationship between X and Y. A value of +1 implies that Y increases as X increases, and vice versa for −1. A value of 0 implies that there is no linear dependency between X and Y. Each spectral measurement is transferred into a vector of X values in its wavelength range. For a VNIR spectrometer, this range is 350 - 2500 nm.

A plot depicting the correlation coefficient versus relative distance is generated to show how correlation relationships varied with geographical distance. The correlation coefficients between each pair of analogue spectral measurements are first calculated. The relative distances between these sampling sites are determined by the GPS record of locations. A scatter plot of the relationship between correlation coefficients and relative distances is then created with the correlation coefficients on the vertical axis and the corresponding relative distances on the horizontal axis.

E. Open Access

The spectral measurements from this trip and future field tests will be published on GitHub with public access, accompanied by the photos of sampling sites and location information. The data and code will be available on GitHub: https://github.com/frankiezoo/hawaii_moon_analogue.

V. Results

The similarity between analogue sampling sites is investigated to assess the consistency of the analogue and the analogue on Mauna Kea is found to be inconsistent with spectral measurements in this frequency range. Some of the sampling sites were revisited during different times of the day to verify the impact of light conditions on measurements. The similarity between analogue sites and lunar reference spectra is then investigated to evaluate the representativeness of the analogue sites considering the mare and highland regions of the lunar surface. The final products of the data analysis are correlation matrices, visualized as heatmaps, containing the correlation coefficients between each pair of sample spectra. The matrix in Fig. 13 and Fig. 14 displays the correlation between each analogue sampling site, while separate matrices in Fig. 16 and Fig. 17 display the correlation between the analogue sampling

sites and reference spectra pulled from publicly available databases. These reference spectra contain data from both returned lunar samples and existing lunar simulants, and a correlation matrix was produced for each category of reference sample. Additionally, Table 1 summarizes the specific analogue field sites that gave the highest correlation coefficient for each reference spectrum. To explore the relationship between correlation and location, a plot of the geographical distance between each pair of analogue sites versus the resulting correlation coefficient is provided shown in Fig. 15. According to the data analysis results, the lunar returned sample and simulants are represented differently by analogue sites. Finally, suggestions are given as to places on the analogue site that best represent the moon spectrally.

The correlation matrices provided a quantitative measure of the relationships between spectra vectors with values ranging from -1 to 1, and the heatmaps visually represented these correlations. Strong positive correlations were indicated by values closer to 1 with darker color, while less correlations were represented by values closer to 0 and negative values with lighter color. A negative correlation usually indicates two variables that tend to move in opposite directions, however, in spectral analysis, it is only showing that the two spectra do not match. This analysis allowed us to identify clusters of measured spectra that exhibited high correlations, representing the high spectral similarity of the corresponding samples.

A. Correlation of Analogue Sampling Sites and Relative Distance

Fig. 13 and Fig. 14 shows the correlations among the measurements taken at the analogue field site. The samples are arranged primarily in order of initial sampling and grouped by sampling site location, so they all begin with abbreviated location and sample number; abbreviated names and an unabbreviated description of the sample can be found in Appendix Table 2. Target spots sampled both in the morning and the afternoon that produced usable spectra are differentiated by “AM” or “PM” designations in the label, but remain grouped with their session ‘group’ - such that those measured in the morning are together and those measured in the afternoon are together. Spots that were chosen for specific characteristics are labeled with abbreviations indicating those characteristics, such as ‘Bk’ or ‘Bw’ for ‘black’ or ‘brown’ regolith, respectively. For the correlation heatmap of the analogue samples, although most of the area is in darker color, representing a high correlation, the values vary from negative to 0.99, indicating that the analogue is not spectrally consistent.

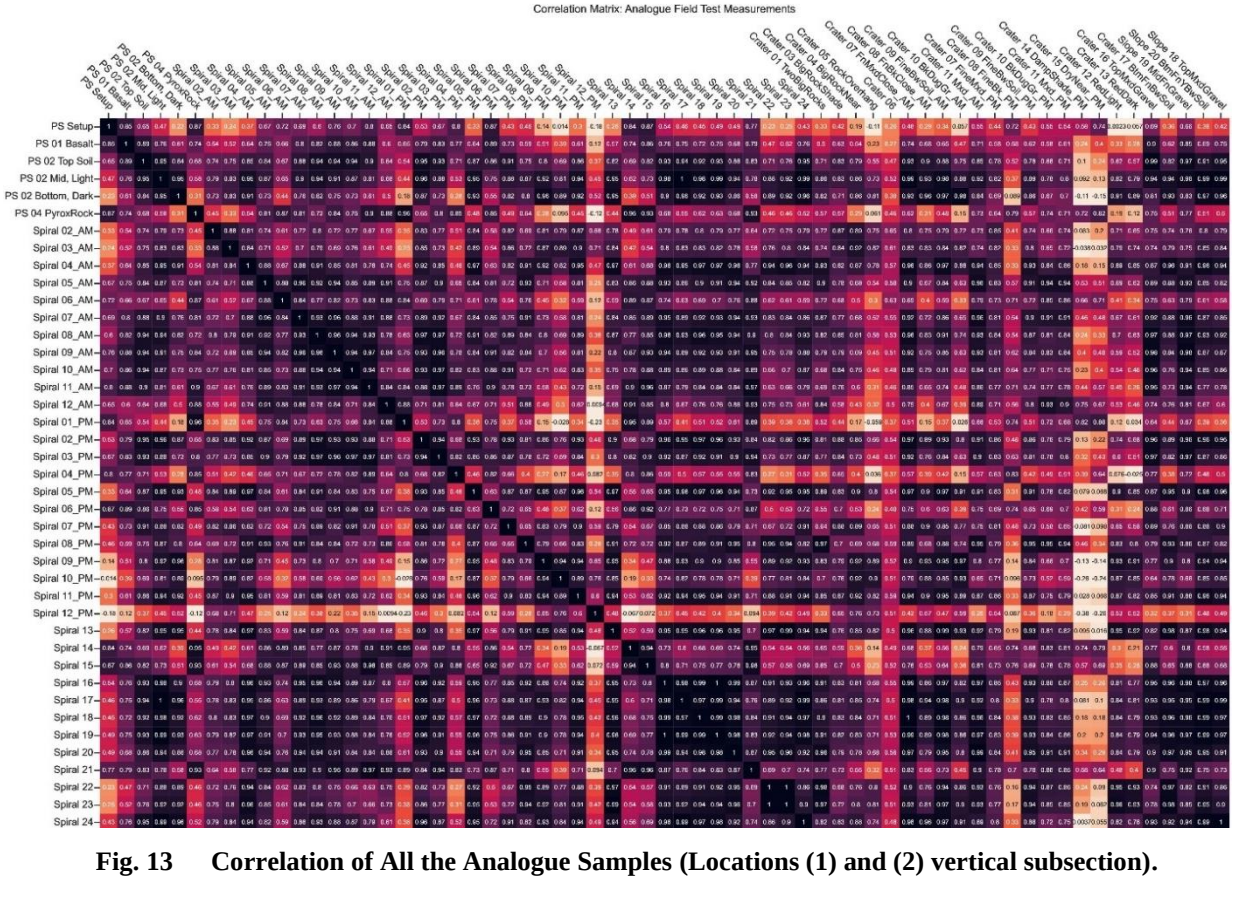

Fig. 13 Correlation of All the Analogue Samples (Locations (1) and (2) vertical subsection).

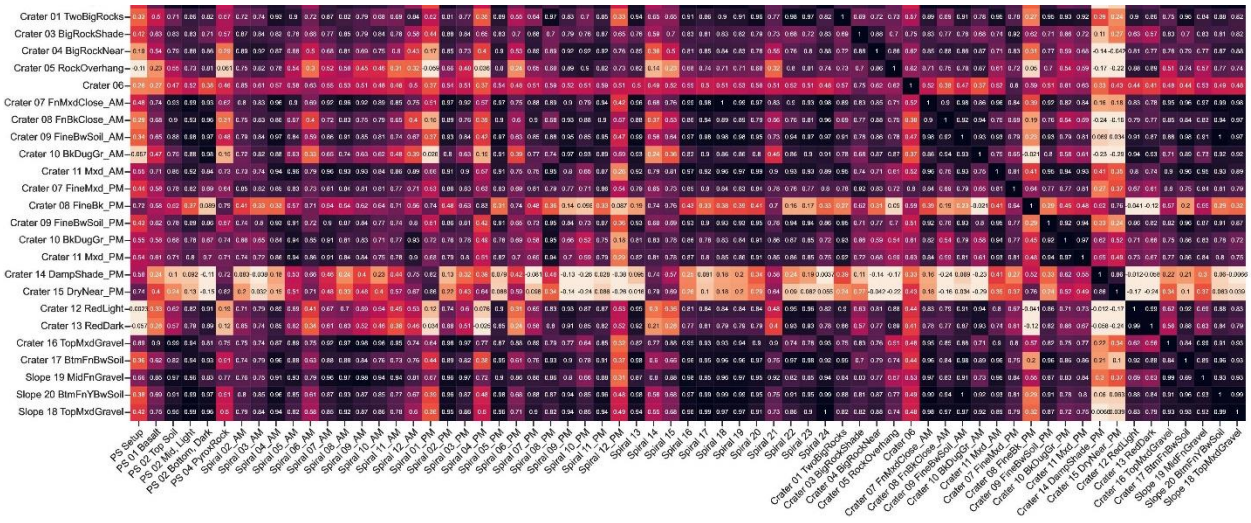

Fig. 14 Correlation of All the Analogue Samples (Locations (3) and (4) vertical subsection).

The analogue sites are for the most part highly correlated with each other with greater than 0.7 correlation coefficients, shown in darker color on the heatmaps. Meanwhile, some outliers (Spots Crater 14 DampShade_PM and Crater 15 DryNear_PM) have very weak correlations with less than 0.6 with most of the other samples, showing they are spectrally different from other sampling spots. Thus, mission operation tests conducted in different areas of the analogue may lead to different performance.

To test the hypothesis that site spectral similarity is correlated to relative distance, Fig. 15 shows correlation coefficients versus relative distance. According to the plot, there is no strong relationship between correlation and geographical distance. Thus, the consistency of the analogue does not depend on the geographical distance. The clustering of data points in high correlation within a short relative distance range may suggest consistency within small areas. However, a few values lower than -0.4 in the short distance range indicate that even locations in close proximity may exhibit significant differences.

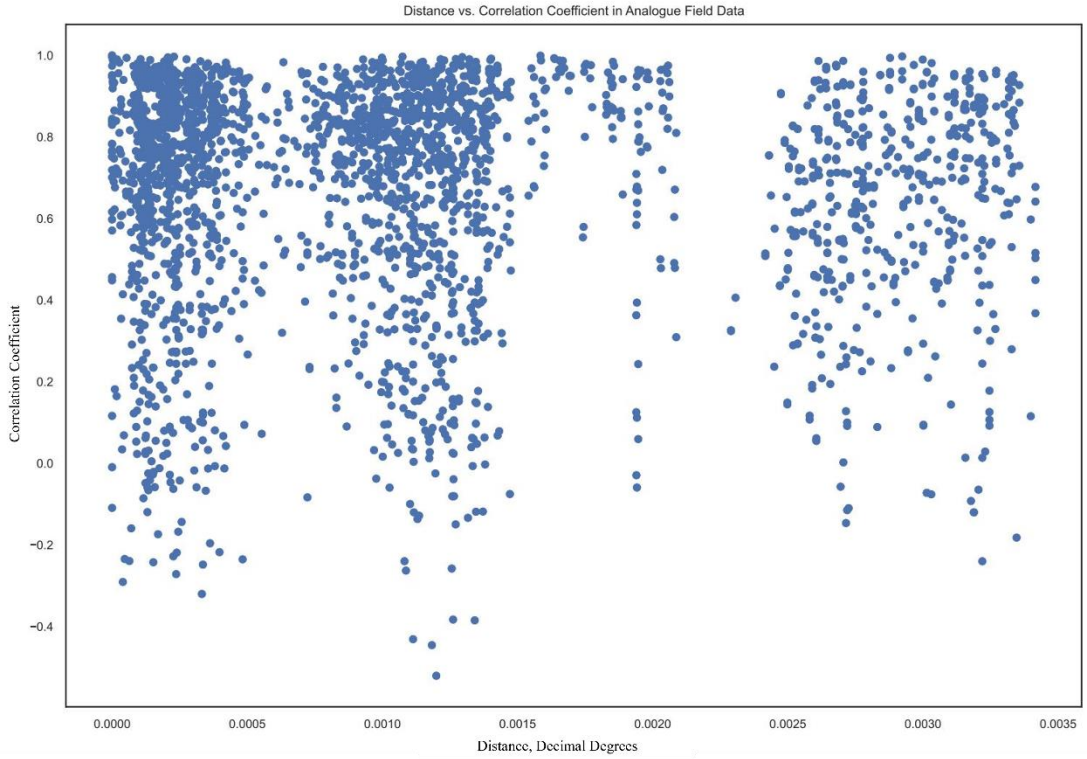

Fig. 15 Geographical Distance vs. Correlation Coefficient scatter plot among Analogue Field Site Samples

B. Correlation of Analogue Samples to Lunar Simulants

Fig. 16 Correlation of Analogue Samples and Lunar Simulants

Fig. 16 is the correlation between analogue measurements and the lunar simulants from the spectral library. This comparison offers insights for future space vehicle and operation tests involving lunar simulants and lunar analogs, highlighting the potential variations in performance. The upper half of Table 1 above displays the analogue sites with the highest correlation with each lunar simulant. Unlike for the lunar returned samples, only half of the selected lunar simulants have a significantly representative analogue site. Highland simulants 3, 4, and 5, and Mare simulant 11 are not well represented by any of the analogue sites in this field test, with no correlation coefficients greater than 0.55. Highland simulant 1, Mare simulant 10, and Basalt simulants 26, and 30 are well represented by the analogue site Crater 10 BkDugGr_AM, with correlation coefficients greater than 0.9. Anorthositic simulant 17 has the highest correlation coefficient of 0.94 with the analogue site Crater 08 FnBkClose_AM, and Anorthositic simulant 31 has the highest correlation coefficient of 0.91 with the analogue site PS 02 Mid, Light.

Furthermore, particle size may also have an impact on representativeness and, consequently, correlation. Among the simulants, Highland simulant 1, Mare simulant 10, Basalt simulant 30, and Anorthositic simulant 31, with particle size distributions ranging from 0 to 1000 micrometers, are found to be well represented by the analogue samples. Anorthositic simulant 17, with a particle size range of 0 to 2000 micrometers, also finds good representation. However, Highland simulants 3, 4, and 5, as well as Mare simulants 11 and 12, with narrower size distributions of under 750 micrometers, are not represented well in this investigation. As a result, it appears that the investigated analogue sites may offer a better representation of lunar regolith with a broader size distribution. In

Fig. 16, the last column representing Anorthositic simulant 17 is in darker color, indicating that this simulant with the widest size distribution has higher correlation coefficients with the analogue measurements compared to the other simulants.

C. Correlation of Analogue Samples to Lunar Samples

Fig. 17 shows the correlation between analogue samples and the lunar returned samples from the spectral library, where abbreviated sample names are defined in Appendix Table 2. The heatmaps discern which sample in the spectral library most accurately represents each analogue sample and which analogue measurement has the highest similarity to each sample in the spectral library. The correlation coefficients range from -0.9 to 0.99, nearly the full range of possible variation. This analogue site represents certain lunar terrain, such as Apollo 11, 14, 16 and 17 sampling sites, better than others, although there is significant difference between analogue and real lunar regolith. When comparing the lunar samples to the analogue measurements, some pairs have significantly higher correlation coefficients than other pairs, such as PS 02 Bottom Dark and Apollo 17 soil sample with a correlation coefficient of 0.99, indicating the analogue site can spectrally represent this lunar terrain very well. The lower half of Table 1 below displays the analogue sites with the highest correlation with each lunar sample. From the table, except for the Apollo 15 Basalt and Apollo 12 RimSoil samples, all the other lunar samples can be represented well by the analogue sites with correlation coefficients higher than 0.9. The site that best represents Apollo 12 mare soil from the rim is the analogue sample PS 04 PyroxRock, with a correlation coefficient of 0.82, while the highest correlation coefficient related to the Apollo 15 Basalt sample is only 0.47. In Fig. 17, it is clear to see that the Apollo 15 Basalt sample is barely represented by any of the analogue sites in this field test. The most noteworthy analogue site is Crater 10 BkDugGr_AM, which has the highest correlation coefficients with all the Apollo 11 mare samples, Apollo 14 highland sample, and most of the Apollo 16 highland samples regardless of the particle size distribution. According to this spectral investigation, the Black gravel dug up and measured in the morning at this sample site can represent Apollo 11, 14, and 16 sampling locations well, although more validation is needed. On the other hand, measurements captured at the same location during different times of the day do not have a correlation of 1, indicating that light conditions exert an influence on the spectral measurements in the field. While Crater 10 BkDugGr_PM and Crater 10 BkDugGr_AM are measurements of the same site taken during different times of the day with different lighting conditions, these site are expected to be highly correlated but the afternoon measurement has lower correlation with the selected lunar samples. The correlation coefficients of the same spot vary from 0.46 to 0.93 with outliers -0.0094 and 0.19. This result could be due to potential errors, which will be discussed later in Limitations.

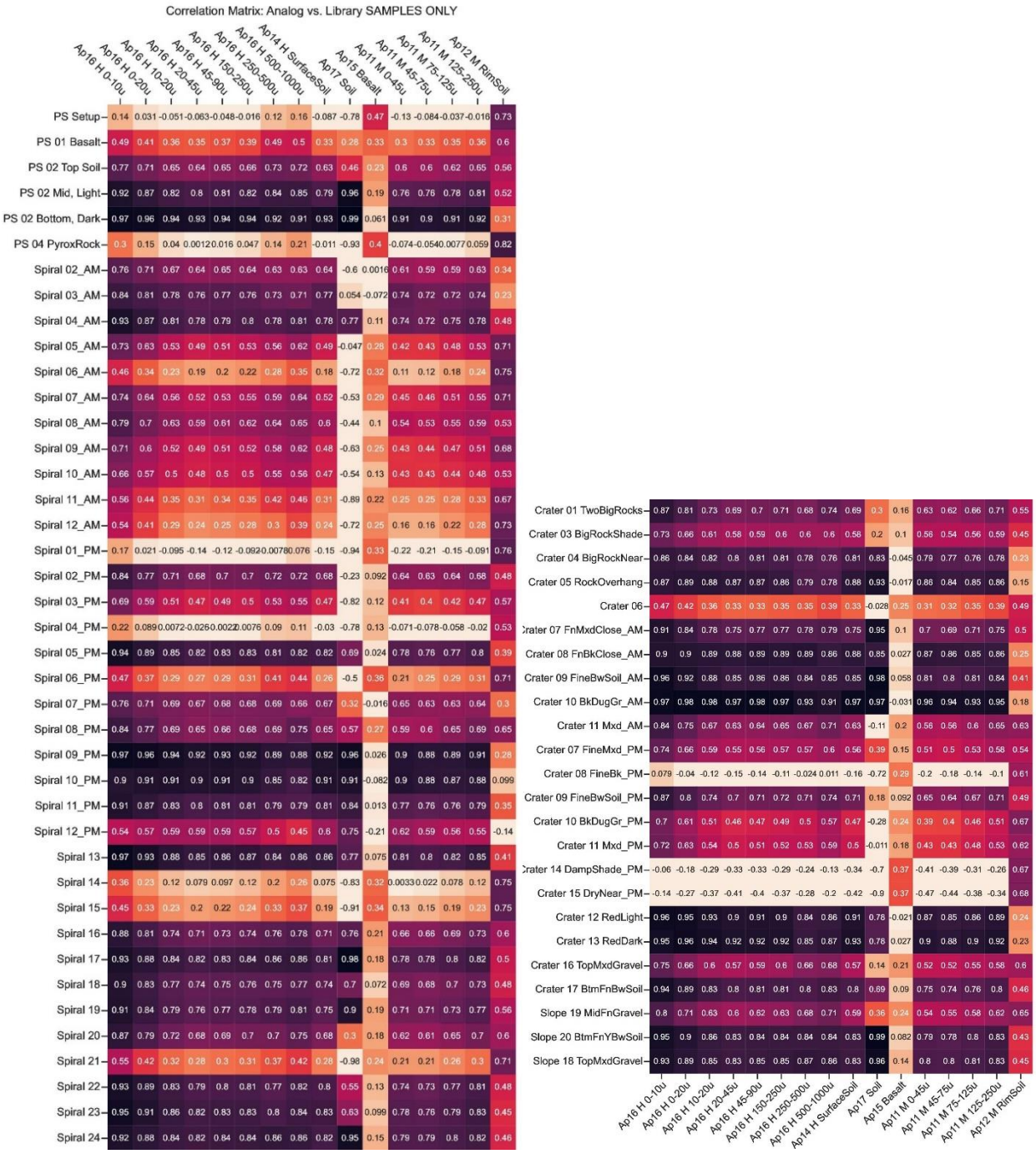

Fig. 17 Correlation of Analogue Samples and Lunar Samples

Table 1 Analogue Field Site w/ Maximum Correlation Coefficient for each Lunar Simulant and Lunar Sample File

Reference Spectra	Analogue Site	Maximum Correlation Coefficient
Sim5 H 0-106u	Crater 08 FnBkClose_AM	0.54
Sim4 H 106-180u	Crater 08 FnBkClose_AM	0.41
Sim3 H 180-750u	Crater 08 FnBkClose_AM	0.39
Sim1 H 0-1000u	Crater 10 BkDugGr_AM	0.93
Sim12 M 106-180u	Crater 08 FnBkClose_AM	0.77
Sim11 M 180-750u	PS 01 Basalt	0.43
Sim10 M 0-1000u	Crater 10 BkDugGr_AM	0.94
Sim30 Ba 0-1000u	Crater 10 BkDugGr_AM	0.94
Sim26 Ba 0-500u	Crater 10 BkDugGr_AM	0.93
Sim31 An 0-1000u	Crater 08 FnBkClose_AM	0.94
Sim17 An 0-2000u	PS 02 Mid, Light	0.91
Ap16 H 0-10u	Crater 10 BkDugGr_AM	0.97
Ap16 H 0-20u	Crater 10 BkDugGr_AM	0.98
Ap16 H 10-20u	Crater 10 BkDugGr_AM	0.98
Ap16 H 20-45u	Crater 10 BkDugGr_AM	0.97
Ap16 H 45-90u	Crater 10 BkDugGr_AM	0.98
Ap16 H 150-250u	Crater 10 BkDugGr_AM	0.97
Ap16 H 250-500u	Crater 10 BkDugGr_AM	0.93
Ap16 H 500-1000u	PS 02 Bottom, Dark	0.91
Ap14 H SurfaceSoil	Crater 10 BkDugGr_AM	0.97
Ap17 Soil	PS 02 Bottom, Dark	0.99
Ap15 Basalt	PS Setup	0.47
Ap11 M 0-45u	Crater 10 BkDugGr_AM	0.96
Ap11 M 45-75u	Crater 10 BkDugGr_AM	0.94
Ap11 M 75-125u	Crater 10 BkDugGr_AM	0.93
Ap11 M 125-250u	Crater 10 BkDugGr_AM	0.95
Ap12 M RimSoil	PS 04 PyroxRock	0.82

According to this analysis, the analogue sites such as Crater 10 BkDugGr_AM and PS 02 Bottom, Dark exhibit spectral similarity to certain lunar surface regions, and are particularly highly correlated with specific lunar spots, such as the Apollo 11, 14, 16, and 17 sampling locations, with correlation coefficients exceeding 0.9.

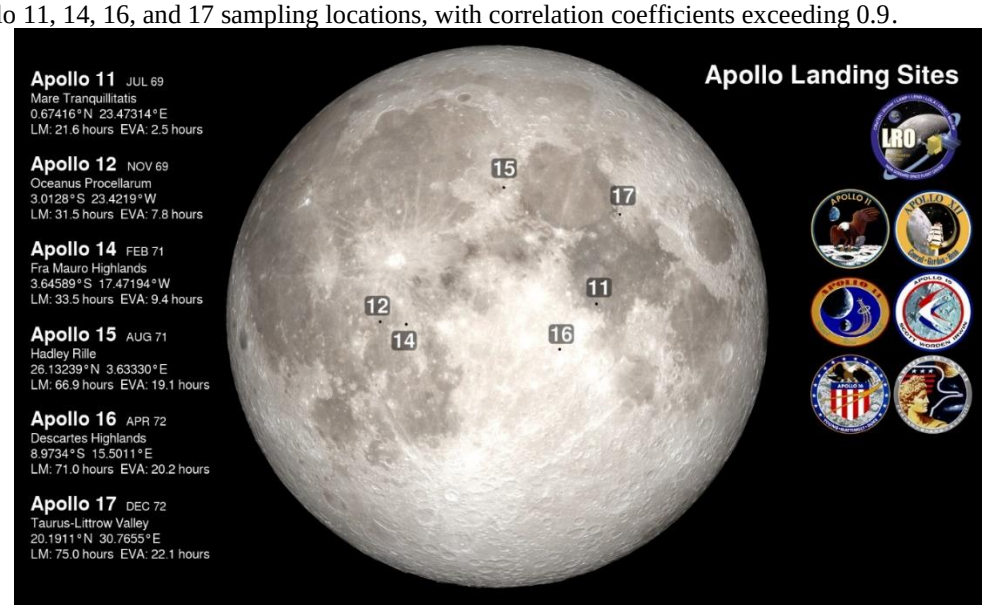

Fig. 18 Apollo Sample Locations [32]

VI. Limitations and Lessons Learned

This section delves into the limitations encountered during this research and the valuable lessons learned from these challenges. Additionally, it explores the potential solutions and improvements for future field investigations.

In the correlation calculation, the amount of data and wavelength range have a significant impact on the results. In our measurements taken in the analogue, there are 1768 points for each field spectra, but the highest count in any of the library files is 356 with various wavelength ranges. The correlation is calculated only based on the overlapping set of wavelengths that both library references and analogue spectra have; higher resolution spectral signatures are not captured.

Among all types of noise, atmospheric noise is one of the most significant ones. Signal processing techniques, such as filtering or signal averaging, are essential to reduce noise in the measurements. However, in a field test under complex environmental conditions, it is still challenging to maintain the signal-to-noise ratio at an optimal level. In our field test, 34 sample measurements were too noisy for analysis, as determined through visual inspection using the ViewSpec graphing tool. The stability and consistency of the light source used for spectral measurements directly influences the accuracy of results. Variations in the intensity or incident angle of the light can introduce systematic errors. Although calibration is done before each measurement, the light condition kept changing during the field test, especially near sunrise and sunset. Crater 10 BkDugGr_PM and Crater 10 BkDugGr_AM, as an example, are the measurements of the same site taken during different times of the day with different lighting conditions, of which the correlation coefficients are not identical.

Human factors, such as instrument operation consistency, can introduce errors too. Variations in instrument setup, sample placement, sampling rate can influence data collection. Implementing standardized protocols and employing a portable removable frame to hold the spectrometer and white reference will help mitigate the effects of human error, rather than the current situation shown in Fig. 10 where they are held by different people. As a preliminary investigation of the analogue and our first field test with the spectrometer, this field trip yielded valuable lessons that will shape our future endeavors. In terms of scheduling, the need to allocate more time for travel, prospecting, and hardware and software debugging is recognised. The team could be divided into the field group and the ground station. The significance of careful site selection and sampling strategies, balancing accessibility and representativeness as well as uniformity and randomness, was also recognised. There will be more options of sampling patterns in addition to the spiral pattern with increased resolution of measurements for different environments in the future tests. Areas with various distributions of water ice, consistent lighting, and minimal organic materials will be prioritized. Thus, sites at higher elevations in winter months would be preferred. Additionally, an ASD contact probe with active lightsource will be an ideal solution to compensate for inadequate and inconsistent light sources. A leveler may be employed to keep a stable and controllable incident angle during sampling on uneven terrain, while the white reference could be mounted to the portable frame along with the spectrometer to avoid shifting as easily in gravel.

VII. Conclusion and Future Work

A. Correlation of Analogue Sampling Sites and Relative Distance

This research conducted spectra-spatial investigation on the Big Island of Hawaii as a lunar surface analogue by collecting spectral measurements to evaluate the consistency of the analogue site and the likeness of the analogue compared to lunar simulants and lunar returned samples based on spectral features. From the correlation matrices, analogue sites that best represent each sample in the spectral library are identified. Data analysis was conducted using correlation matrices to reveal patterns within the datasets.

According to the correlation matrix of analogue samples in Fig. 13 and Fig. 14, although most of the area is in darker color, representing a high correlation, the values vary. The spectral measurements in the analogue are not consistent and the correlation does not depend on the relative distance. The measurements captured at the same location during different times of the day do not have a correlation of 1, indicating that light conditions exert an influence on the spectral measurements in the field. According to the correlation matrices Fig. 16 and Fig. 17, it is possible to discern which analogue measurement has the highest similarity to any lunar returned sample or lunar simulants in the spectral library. The lunar samples and simulants can be most accurately represented by the analogue sites with the highest correlation coefficients. Among the investigated sites, Crater 10 BkDugGr_AM can represent Apollo 11, 14, and 16 samples well with high correlation values ranging from 0.93 to 0.98. However, not all the lunar samples and simulants can be well represented by the analogue measurements. Apollo 15 Basalt sample, Highland simulant 3, 4, and 5, do not exhibit a high similarity to any of the sampling analogue sites, as indicated by correlation coefficients less than 0.6.

B. Future Work

To directly investigate similarity of the planetary analogue to icy mixtures in the lunar south pole region, spectra of icy regolith in the analogue will be measured and correlated to the remote sensing spectral data from past lunar missions, such as Moon Mineralogy Mapper (M3), as well as to the measurements of icy mixtures produced in the lab. The correlation between analogue measurements and the measurements of lunar samples from Apollo missions will be discussed to better understand the similarity between terrestrial analogue and specific lunar locations. Additionally, incorporating automation for data collection and processing to streamline the workflow is part of our future plans, enabling automatic logging of site location, time, and data collected. Acknowledging the limitations of GPS accuracy, both GPS and GLONASS positions will be recorded for improved location precision. Furthermore, an investigation procedure to evaluate the lunar surface analogue can be expanded to other planetary surface analogues and contribute to more future space missions.

Appendix

Table 2 Analogue Field and Reference Library Data Name Codes and Descriptions

LABEL	DESCRIPTION
Analogue Field Data	
'PSxxx'	**Location (1) Power Station**
PS Setup	Setup Area
PS 01 BasaltShade	Spot #01, Basalt, Shade under rock
PS 02 TopSoil	Spot #02, Soil Layers - Top
PS 02 MidLight	Spot #02, Soil Layers - Middle, Light-colored
PS 02 BottomDark	Spot #02, Soil Layers - Bottom, Dark-colored
PS 04 PyroxRock	Spot #04 Rock, Pyroxene Xenolith
'Spiralxxx'	**Location (2) Between Two Cinder Cones**
Spiral 02_AM	Spot #02, Spiral Pattern, Morning
Spiral 03_AM	Spot #03, Spiral Pattern, Morning
Spiral 04_AM	Spot #04, Spiral Pattern, Morning
Spiral 05_AM	Spot #05, Spiral Pattern, Morning
Spiral 06_AM	Spot #06, Spiral Pattern, Morning
Spiral 07_AM	Spot #07, Spiral Pattern, Morning
Spiral 08_AM	Spot #08, Spiral Pattern, Morning
Spiral 09_AM	Spot #09, Spiral Pattern, Morning
Spiral 10_AM	Spot #10, Spiral Pattern, Morning
Spiral 11_AM	Spot #11, Spiral Pattern, Morning
Spiral 12_AM	Spot #12, Spiral Pattern, Morning
Spiral 01_PM	Spot #01, Spiral Pattern, Dusk
Spiral 02_PM	Spot #02, Spiral Pattern, Dusk
Spiral 03_PM	Spot #03, Spiral Pattern, Dusk
Spiral 04_PM	Spot #04, Spiral Pattern, Dusk
Spiral 05_PM	Spot #05, Spiral Pattern, Dusk
Spiral 06_PM	Spot #06, Spiral Pattern, Dusk
Spiral 07_PM	Spot #07, Spiral Pattern, Dusk
Spiral 08_PM	Spot #08, Spiral Pattern, Dusk
Spiral 09_PM	Spot #09, Spiral Pattern, Dusk
Spiral 10_PM	Spot #10, Spiral Pattern, Dusk

Spiral 11_PM	Spot #11, Spiral Pattern, Dusk
Spiral 12_PM	Spot #12, Spiral Pattern, Dusk
Spiral 13	Spot #13, Grid Pattern
Spiral 14	Spot #14, Grid Pattern
Spiral 15	Spot #15, Grid Pattern
Spiral 16	Spot #16, Grid Pattern
Spiral 17	Spot #17, Grid Pattern
Spiral 18	Spot #18, Grid Pattern
Spiral 19	Spot #19, Grid Pattern
Spiral 20	Spot #20, Grid Pattern
Spiral 21	Spot #21, Grid Pattern
Spiral 22	Spot #22, Grid Pattern
Spiral 23	Spot #23, Grid Pattern
Spiral 24	Spot #24, Grid Pattern
'Craterxxx'	**Location (3) Crater Bed**
Crater 01 TwoBigRocks	Spot #01, Between Two Big Rocks
Crater 02	Spot #02
Crater 03 BigRockShade	Spot #03, Under Big Rock, Shaded
Crater 04 BigRockNear	Spot #04, Near Big Rock, Open Area
Crater 05 RockOverhang	Spot #05, Under a Rock Overhang
Crater 06	Spot #06
Crater 07 FnMxdClose_AM	Spot #07, Fine Sand, Mixed Brown/Black, Similar nearby to original #07, Morning
Crater 08 FnBkClose_AM	Spot #08, Fine Sand, Black, Nearby location to original #08, Morning
Crater 09 FineBwSoil_AM	Spot #09, Fine Brown Soil Dug from Under Top Gravel, Morning
Crater 10 BkDugGr_AM	Spot #10, Very Black Gravel Dug from Under Brown Soil, Morning
Crater 11 Mxd_AM	Spot #11, Mixture of Brown Soil & Black Gravel (#10 & #11), Morning
Crater 14 DampShade_AM	Spot #14, Damp Soil Under Rock Overhang, Morning
Crater 15 DryNear_AM	Spot #15, Dry Soil of Similar Color Near #14 Damp Soil, Morning
Crater 07 FineMxd_PM	Spot #07, Fine Sand, Mixed Brown/Black, Dusk
Crater 08 FineBk_PM	Spot #08, Fine Sand, Black, Dusk
Crater 09 FineBwSoil_PM	Spot #09, Fine Brown Soil Dug from Under Top Gravel, Dusk
Crater 10 BkDugGr_PM	Spot #10, Very Black Gravel Dug from Under Brown Soil, Dusk
Crater 11 Mxd_PM	Spot #11, Mixture of Brown Soil & Black Gravel (#10 & #11), Dusk
Crater 14 DampShade_PM	Spot #14, Damp Soil Under Rock Overhang, Dusk
Crater 15 DryNear_PM	Spot #15, Dry Soil of Similar Color Near #14 Damp Soil, Dusk
Crater 12 RedLight	Spot #12, Red Rock 1, Lighter
Crater 13 RedDark	Spot #13, Red Rock 2, Darker
Crater 16 TopMxdGravel	Spot #16, Upper Layer, Mixed Gravel
Crater 17 BtmFnBwSoil	Spot #17, Bottom Layer, Brown Fine Soil
'Slopexxx'	**Location (4) Crater Side**
Slope 19 MidFnGravel	Spot #19, Middle Layer, Finer Gravel
Slope 20 BtmFnYBwSoil	Spot #20, Bottom Layer, Fine Soil, Light-colored (Yellow/Brown)

Slope 18 TopMxdGravel	Spot #18, Top Layer, Top Mixed Gravel
Reference Library Data	
Sim5 H 0-106u	Simulant #5, Highland, 0-106um
Sim4 H 106-180u	Simulant #4, Highland, 106-180um
Sim3 H 180-750u	Simulant #3 Highland, 180-750um
Sim1 H 0-1000u	Simulant #1, Highland, 0-1000um
Sim12 M 106-180u	Simulant #12, Mare, 106-180um
Sim11 M 180-750u	Simulant #11, Mare, 180-750um
Sim10 M 0-1000u	Simulant #10, Mare, 0-1000um
Sim30 Ba 0-1000u	Simulant #30, Basaltic, 0-1000um
Sim26 Ba 0-500u	Simulant #26, Basaltic, 0-500um
Sim31 An 0-1000u	Simulant #31, Anorthositic, 0-1000um
Sim17 An 0-2000u	Simulant #17, Anorthositic, 0-2000um
Ap16 H 0-10u	Apollo 16 Sample, Highland, 0-10um
Ap16 H 0-20u	Apollo 16 Sample, Highland, 0-20m
Ap16 H 10-20u	Apollo 16 Sample, Highland, 10-20m
Ap16 H 20-45u	Apollo 16 Sample, Highland, 20-45m
Ap16 H 45-90u	Apollo 16 Sample, Highland, 45-90m
Ap16 H 150-250u	Apollo 16 Sample, Highland, 150-250um
Ap16 H 250-500u	Apollo 16 Sample, Highland, 250-500um
Ap16 H 500-1000u	Apollo 16 Sample, Highland, 500-1000um
Ap14 H SurfaceSoil	Apollo 14 Sample, Highland, Surface Soil
Ap17 Soil	Apollo 17 Sample, Soil
Ap15 Basalt	Apollo 15 Sample, Basalt
Ap11 M 0-45u	Apollo 11 Sample, Mare, 0-45um
Ap11 M 45-75u	Apollo 11 Sample, Mare, 45-75um
Ap11 M 75-125u	Apollo 11 Sample, Mare, 75-125um
Ap11 M 125-250u	Apollo 11 Sample, Mare, 125-250um
Ap12 M RimSoil	Apollo 12 Sample, Mare, Crater Rim Soil

Acknowledgments

This work was supported by NASA Grant HI-80NSSC21M0334 and the Hawai‘i Space Grant Consortium. We would like to express our heartfelt gratitude to Dr. Shuai Li (The Hawai‘i Institute of Geophysics and Planetology, University of Hawai‘i at Mānoa) and his dedicated graduate student, Nina de Castro (The Hawai‘i Institute of Geophysics and Planetology, University of Hawai‘i at Mānoa), for their invaluable assistance and expertise for our analogue field test. Their support and guidance significantly enhanced the quality and efficiency of our research.

References

[1] Li, S., Lucey, P. G., Milliken, R. E., Hayne, P. O., Fisher, E., Williams, J.-P., Hurley, D. M., and Elphic, R. C., “Direct evidence of surface exposed water ice in the lunar polar regions,” *Proceedings of the National Academy of Sciences*, vol. 115, 2018, pp. 8907–8912.

[2] Meirion-Griffith, G. and Spenko, M. "A new pressure-sinkage model for small, rigid wheels on deformable terrains." *Proceedings of the Joint 9th Asia-Pacific ISTVS Conference and Annual Meeting of Japanese Society for Terramechanics*, vol. 27, International Society for Terrain-Vehicle Systems, Sapporo, Japan, September 2010.

[3] U.S. Geological Survey (USGS). 2015. USGS 10-m Digital Elevation Model (DEM): Hawaii: Big Island. Distributed by the Pacific Islands Ocean Observing System (PacIOOS). http://pacioos.org/metadata/usgs_dem_10m_bigisland.html. Accessed [retrieved 26 March 2023].

[4] Romo, R., Andersen, C., Edison, K., and Musilova, M. "Analog Field Sites on Hawai'i Island." In *Earth and Space 2021*, American Society of Civil Engineers, 2021, pp. 577-589.
[5] Edison, K., Andersen, C., Harford, K., Tokunaga, J. and Romo, R. "The Effects of Mineral Abundances on Mechanical and Structural Properties of Sintered Hawaiian Basalt Aggregate: Implications for Lunar/Mars ISRU Applications." In *Earth and Space 2021*, American Society of Civil Engineers, 2021, pp. 818-831
[6] McKyes, E. and Fan, T. "Multiplate penetration tests to determine soil stiffness moduli," *Journal of Terramechanics*, vol. 22, no. 3, 1985, pp. 157-162.
[7] Lucey, P. G., Petro, N., Hurley, D. M., Farrell, W. M., Prem, P., Costello, E. S., ... & Orlando, T. (2022). Volatile interactions with the lunar surface. Geochemistry, 82(3), 125858.
[8] National Aeronautics and Space Administration (2023, June 7). VIPER: The Rover and Its Onboard Toolkit. Retrieved June 24, 2023, from https://www.nasa.gov/viper/rover
[9] Edison, K., Andersen, C., Harford, K., Higaki, K., & Romo, R. (2019). Hawaiian basalt characterization and the effects of chemical composition variances on the sintering process; Potential implications for Lunar/Mars ISRU applications. In International astronautical conference.
[10] Yingst, R. A., Russell, P., Ten Kate, I. L., Noble, S., Graff, T., Graham, L. D., & Eppler, D. (2015). Designing remote operations strategies to optimize science mission goals: lessons learned from the Moon Mars Analog Mission Activities Mauna Kea 2012 field test. Acta Astronautica, 113, 120-131.
[11] Ito, G., Rogers, A. D., Young, K. E., Bleacher, J. E., Edwards, C. S., Hinrichs, J., ... & Glotch, T. D. (2018). Incorporation of portable infrared spectral imaging into planetary geological field work: analog studies at Kīlauea Volcano, Hawaii, and Potrillo Volcanic Field, New Mexico. Earth and Space Science, 5(11), 676-696.
[12] Ten Kate, I. L., Armstrong, R., Bernhardt, B., Blumers, M., Craft, J., Boucher, D., ... & Zacny, K. (2013). Mauna Kea, Hawaii, as an analog site for future planetary resource exploration: results from the 2010 ILSO-ISRU field-testing campaign. Journal of Aerospace Engineering, 26(1), 183-196.
[13] Elphic, R. C., Heldmann, J. L., Marinova, M. M., Colaprete, A., Fritzler, E. L., McMurray, R. E., ... & Smith, T. F. (2015). Simulated real-time lunar volatiles prospecting with a rover-borne neutron spectrometer. Advances in Space Research, 55(10), 2438-2450.
[14] Sanders, G. B., Larson, W. E., Picard, M., & Hamilton, J. C. (2011, January). Use of Hawaii analog sites for lunar science and in-situ resource utilization. In 2011 European Planetary Science Congress (EPSC) and the American Astronomical Society"s Division of Planetary Sciences (DPS)(EPSC-DPS 2011) (No. JSC-CN-24415).
[15] Gwizd, S., Stack, K. M., Calef, F., Francis, R., Tolometti, G., Graff, J., Langley, C., Kristinsson, Þ. H., Thorarensen, V. P., Bernharðsson, E., Phillips, M., Moersch, J., Basu, U., Voigt, J. R. C., & Hamilton, C. W. (2023). Rover-Aerial Vehicle Exploration Network (RAVEN): Mission Planning, Implementation, and Results from the 2022 Rover-Only Field Campaign at Holuhraun, Iceland. In the 54th Lunar and Planetary Science Conference.
[16] Bakeev, K. A., & Chimenti, R. V. (2013). Pros and cons of using correlation versus multivariate algorithms for material identification via handheld spectroscopy. Am. Pharm. Rev, 16(10).
[17] Henschel, H., & Van der Spoel, D. (2020). An intuitively understandable quality measure for theoretical vibrational spectra. The Journal of Physical Chemistry Letters, 11(14), 5471-5475.
[18] Henschel, H., Andersson, A. T., Jespers, W., Mehdi Ghahremanpour, M., & Van der Spoel, D. (2020). Theoretical infrared spectra: quantitative similarity measures and force fields. Journal of Chemical Theory and Computation, 16(5), 3307-3315.
[19] Imai, F. H., Rosen, M. R., & Berns, R. S. (2002, January). Comparative study of metrics for spectral match quality. In Conference on colour in graphics, imaging, and vision (Vol. 2002, No. 1, pp. 492-496). Society for Imaging Science and Technology.
[20] Milliken, R. (2020). The RELAB Spectral Library Bundle contains reflectance spectra and ancillary data acquired at the Reflectance Experiment Laboratory (RELAB) at Brown University. https://doi.org/10.17189/1519032.
[21] Kokaly, R.F., Clark, R.N., Swayze, G.A., Livo, K.E., Hoefen, T.M., Pearson, N.C., Wise, R.A., Benzel, W.M., Lowers, H.A., Driscoll, R.L., and Klein, A.J. (2017). USGS Spectral Library Version 7: U.S. Geological Survey Data Series 1035, 61 p., https://doi.org/10.3133/ds1035.
[22] Lu, X., Chen, J., Ling, Z., Liu, C., Fu, X., Qiao, L., ... & Xu, R. (2023). Mature lunar soils from Fe-rich and young mare basalts in the Chang'e-5 regolith samples. Nature Astronomy, 7(2), 142-151.
[23] Chen, J., Ling, Z., Qiao, L., He, Z., Xu, R., Sun, L., ... & Qi, X. (2020). Mineralogy of Chang'e-4 landing site: Preliminary results of visible and near-infrared imaging spectrometer. *Science China Information Sciences*, *63*, 1-12.
[24] Liu, B., Ren, X., Yan, W., Xu, X., Cai, T., Liu, D., ... & Li, C. (2016, April). Detection Capability Evaluation on Chang'e-5 Lunar Mineralogical Spectrometer (LMS). In EGU General Assembly Conference Abstracts (pp. EPSC2016-5644).
[25] Li, H., Liu, B., Ren, X., Liu, J., Li, C., Xu, X., ... & Tian, M. (2015, December). Ground Verification Test of Lunar Mineralogical Spectrometer on the Chang'e 5 Lunar Sample Return Lander. In AGU Fall Meeting Abstracts (Vol. 2015, pp. P11B-2076).
[26] Spudis, P. D., Plescia, J. B., Bussey, D. B. J., Josset, J. L., & Beauvivre, S. (2008, March). The geology of the south pole of the Moon and age of Shackleton crater. In 39th Annual Lunar and Planetary Science Conference (No. 1391, p. 1626).
[27] Wilhelms, D. E., Howard, K. A., & Wilshire, H. G. (1979). Geologic map of the south side of the Moon. Department of the Interior, US Geological Survey.
[28] Gawronska, A. J., Barrett, N., Boazman, S. J., Gilmour, C. M., Halim, S. H., McCanaan, K., ... & Kring, D. A. (2020). Geologic context and potential EVA targets at the lunar south pole. Advances in Space Research, 66(6), 1247-1264.

[29] Peterson, C. A., Hawke, B. R., Lucey, P. G., Taylor, G. J., Blewett, D. T., & Spudis, P. D. (1997, March). Lunar anorthosite: identification and distribution of remnants of the primordial crust. In Lunar and Planetary Science Conference (p. 1097).
[30] Uemoto, K., Ohtake, M., Haruyama, J., Matsunaga, T., Yokota, Y., Morota, T., ... & Iwata, T. (2010, March). Purest anorthosite distribution in the lunar South Pole-Aitken basin derived from SELENE multiband imager. In 41st Annual Lunar and Planetary Science Conference (No. 1533, p. 1635).
[31] ASD Inc. (2016, May). FieldSpec®4 User Manual. ASD Inc.
[32] Wright, E., & Petro, N. (2019). Apollo landing sites with moon phases. NASA's Scientific Visualization Studio. Retrieved September 23, 2023, from https://svs.gsfc.nasa.gov/4731.

Revised September 2023